

Fig. 3 Flight-test base pressure data,  $R_n/R_b = 0.3$ .

on the RV was verified by telemetered heatshield calorimeter data. Note that  $Re_{e,L}$  varies from  $1.9 \times 10^6$  to  $6.3 \times 10^6$  and is, owing to the bluntness of this vehicle, only about 10% of the corresponding  $Re_{\infty,L}$ . Because the  $Re_{e,L}$  is considerably less than  $4 \times 10^7$ , a significant Reynolds-number effect is expected on the basis of the Whitfield and Potter conclusions.

High-Reynolds-number predictions<sup>1,3</sup> for the  $M_\infty = 10.5$  data are also included in Fig. 3. Reasons for the discrepancy between these two semiempirical predictions have been discussed by Cassanto and Mendelson;<sup>11</sup> hence, it suffices only to point out that both methods indicate a base pressure level considerably lower than what was in fact measured. The rather severe variation ( $\sim 60\%$ ) in  $p_b/p_e$  seen for  $Re_{e,L} \leq 6.3 \times 10^6$  illustrates the Reynolds-number influence on a full-scale hypersonic flight vehicle.

#### Conclusions

The influence of Reynolds number on turbulent base pressure has been discussed relative to hypersonic re-entry. Flight data from slightly blunt slender cones, for which  $Re_{e,L} \gg 4 \times 10^7$  ( $Re_{e,L} \approx 2Re_{\infty,L}$ ), reveal no Reynolds-number effect, whereas an appreciable Reynolds-number dependence ( $\sim 60\%$  variation) is shown for a very blunt slender cone for which  $Re_{e,L} \ll 4 \times 10^7$  ( $Re_{e,L} \approx 0.1 Re_{\infty,L}$ ). These hypersonic ( $M_\infty \approx 15$  and  $10.5$ ) results are consistent with the ground-test data of Whitfield and Potter for  $M_\infty = 2-5$  and support the conclusion that, unless  $Re_{e,L}$  is sufficiently large, Reynolds-number variations may strongly influence the turbulent base pressure of full-scale vehicles during re-entry.

#### References

- Whitfield, J. D. and Potter, J. L., "On Base Pressures at High Reynolds Numbers and Hypersonic Mach Numbers," AEDC-TN-60-61, March 1960, Arnold Engineering Development Center, Tullahoma, Tenn.
- Zarin, N. A., "Base Pressure Measurements on Sharp and Blunt  $9^\circ$  Cones at Mach Numbers from 3.50 to 9.20," *AIAA Journal*, Vol. 4, No. 4, April 1966, pp. 743-745.
- Cassanto, J. M., "Effect of Cone Angle and Bluntness Ratio on Base Pressure," *AIAA Journal*, Vol. 3, No. 12, Dec. 1965, pp. 2351-2352.
- Cassanto, J. M. and Storer, E. M., "A Revised Technique for Predicting the Base Pressure of Sphere Cone Configurations in Turbulent Flow Including Mass Addition Effects," ALFM 68-41, Oct. 1968, Re-Entry Systems Dept., General Electric Co., Philadelphia, Pa.
- Cassanto, J. M. and Hoyt, T. L., "Flight Results Showing the Effect of Mass Addition on Base Pressure," *AIAA Journal*, Vol. 8, No. 9, Sept. 1970, pp. 1705-1707.
- Bulmer, B. M., "Effect of Low Heat-Shield Ablation Rates on Flight Test Turbulent Base Pressure," *AIAA Journal*, Vol. 10, No. 12, Dec. 1972, pp. 1704-1705.
- Cassanto, J. M., "Base Pressure Results at  $M = 4$  Using Free-Flight and Sting-Supported Models," *AIAA Journal*, Vol. 6, No. 7, July 1968, pp. 1411-1414.

<sup>8</sup> Hayos, F. G., "Turbulent Boundary-Layer Effects on Base Pressure," *Journal of the Aeronautical Sciences*, Vol. 24, No. 10, Oct. 1957, pp. 781-782.

<sup>9</sup> Hochrein, G. J., "A Procedure for Computing Aerodynamic Heating on Sphere Cones—Program BLUNTY," SC-DR-69-449, Nov. 1969, Sandia Labs., Albuquerque, N. Mex.

<sup>10</sup> Cassanto, J. M., "Flight Test Base Pressure Results at Hypersonic Mach Numbers in Turbulent Flow," *AIAA Journal*, Vol. 10, No. 3, March 1972, pp. 329-331.

<sup>11</sup> Cassanto, J. M. and Mendelson, R. S., "Local Flow Effects on Base Pressure," *AIAA Journal*, Vol. 6, No. 6, June 1968, pp. 1182-1185.

## Spherically-Symmetric Supersonic Source Flow: A New Use For The Prandtl-Meyer Function

WALTER F. REDDALL III\*

The Aerospace Corporation, El Segundo, Calif.

#### Introduction

INVISCID supersonic flow with spherical symmetry is so simple that it seems to deserve more attention than it has been given in most textbooks on gas dynamics. This is particularly true in light of the fact that investigators who study the plume generated by a rocket exhaust frequently appeal to supersonic source flow as the limit reached by the flow far downstream of the nozzle, and also as a simplification of the flow in the nozzle itself near the exit plane.

The conditions in a conical, divergent nozzle of half-angle  $\theta_N$  need not be uniform in the conical coordinate  $\theta$ , but when the assumption is made that they are, the dependent variables become functions only of the radial coordinate  $R$ , measured from the virtual origin of the cone. In this case the flow bounded by the nozzle wall fits the requirements of quasi-one-dimensional isentropic motion. The streamlines in such a flow are radial lines, and the flow can only exist in the domain  $R > R^*$ , where  $R^*$  is the radius at which sonic conditions exist (c.f. Courant and Friedrichs, pp. 377-380). The characteristics, however, are curves in  $(R, \theta)$  space (see Fig. 1), the equations for which are not well documented, if at all. This Note presents a derivation of those equations for the case of a perfect gas, using the local Mach number as a curve parameter. A generalization to any real gas is also provided. The results reveal that the change in streamline slope  $\theta$  between any two points on a characteristic is equal to half the change in the Prandtl-Meyer function between the same two points. This is in contrast to the case of radial supersonic flow in a plane, where the change in  $\theta$  along a physical characteristic is equal to the change in Prandtl-Meyer function. (The image of such a radial-flow characteristic in the hodograph plane is an epicycloid of the same family.) The connection thus established between a function thought to have application only to plane flows and a spherically-symmetric flow is the most interesting feature of the analysis.

The exact relations for the characteristics may be valuable, as are most exact solutions, as a standard for measuring the error of approximate solutions. For example, a method-of-characteristics computer code could be given the simple task of computing a conical flow starting from a set of exact conditions at some initial station  $R_i$  and the departure of the computed

Received July 12, 1973; revision received August 13, 1973.

Index category: Supersonic and Hypersonic Flow.

\* Member of Technical Staff.

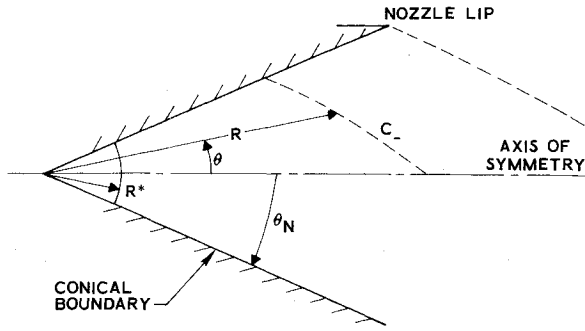


Fig. 1 Spherically symmetric flow in a conical nozzle.

characteristics from the true location after a given number of cycles could be used as a guide to the error associated with a particular choice of mesh size.

If a conical nozzle is underexpanded, then for a given radial position  $R_L$  of the lip, the characteristic that would leave the nozzle boundary at  $R_L$  if there were no lip is the first characteristic in the expansion wave through which the flow adjusts to external conditions. A knowledge of the properties along this curve may be useful in seeking alternative local coordinate systems in which to analyze the expansion region.

#### Analysis

Consider a spherically-symmetric supersonic flow of a perfect gas directed radially outward in the domain  $R > R^*$ ,  $0 \leq \theta \leq \theta_N$ . For this one-dimensional flow the familiar area-Mach number relation holds:

$$\frac{A}{A^*} = \frac{1}{M} \left[ \frac{2}{\gamma+1} \left( 1 + \frac{\gamma-1}{2} M^2 \right) \right]^{(\gamma+1)/2(\gamma-1)} \quad (1)$$

where  $A^* = 2\pi(1 - \cos \theta_N)R^{*2}$  is the section of a spherical surface of radius  $R^*$  cut out by a cone of half-angle  $\theta_N$ , and  $A$  is the corresponding area at an arbitrary coordinate  $R > R^*$ . If we take the square root of Eq. (1), the result:

$$\frac{R}{R^*} = M^{-1/2} \left[ \frac{2}{\gamma+1} \left( 1 + \frac{\gamma-1}{2} M^2 \right) \right]^{(\gamma+1)/4(\gamma-1)} \quad (2)$$

gives the Mach number implicitly as a function of  $R$ . Alternatively, the expression (2) gives the radial coordinate  $R$  along any curve  $R(\xi)$ ,  $\theta(\xi)$  if we identify the Mach number with the curve parameter  $\xi$ . This is permissible, because for the supersonic branch of the function (1) the Mach number is known to increase monotonically from  $1.0 \rightarrow \infty$  with increasing area ratio. (See Liepmann & Roshko, Fig. 5.2).

In particular, the characteristic curves  $C_+$  or  $C_-$  can be described parametrically if a second relation  $\theta(M)$  can be found which distinguishes them from any other curve, and which complements Eq. (2). Such a relation is given by the slope of the characteristics, measured with respect to the axis of symmetry:

$$\tan(\theta \pm \mu) = \frac{\sin \theta dR + R \cos \theta d\theta}{\cos \theta dR - R \sin \theta d\theta} \quad (3)$$

where the Mach angle  $\mu$  is given by

$$\mu = \arctan(M^2 - 1)^{-1/2} \quad (4)$$

After some manipulation Eq. (3) reduces to

$$d\theta = \pm \tan \mu d \ln R \quad (5)$$

Now if we integrate Eq. (5) along the characteristic from some initial point, we obtain

$$\theta - \theta_0 = \pm \int_{M_0}^M (M^2 - 1)^{-1/2} \cdot \frac{d \ln R}{dM} \cdot dM \quad (6)$$

The logarithmic derivative occurring in the integrand is obtained from Eq. (2):

$$\frac{d \ln R}{dM} = \frac{M^2 - 1}{2M \{1 + [(\gamma-1)/2]M^2\}}$$

so that

$$\theta - \theta_0 = \pm \frac{1}{2} \int_{M_0}^M \frac{(M^2 - 1)^{1/2}}{\{1 + [(\gamma-1)/2]M^2\}} \frac{dM}{M} \quad (7)$$

But this integral is simply the Prandtl-Meyer function,  $v(M)$ .

$$v(M) = \left( \frac{\gamma+1}{\gamma-1} \right)^{1/2} \arctan \left[ \frac{\gamma-1}{\gamma+1} (M^2 - 1) \right]^{1/2} - \arctan [M^2 - 1]^{1/2} \quad (8)$$

Thus we have the remarkable result that for a spherically-symmetric supersonic flow the change in slope of a streamline along a characteristic measured from a reference condition is given by one-half of the change in the Prandtl-Meyer function between the two locations:

$$\theta - \theta_0 = \pm \frac{1}{2} [v(M) - v(M_0)] \quad (9)$$

In the case of plane radial flow, where the areas are proportional to  $R$ , the factor  $\frac{1}{2}$  disappears, leaving the familiar planar relation between streamline slope and Prandtl-Meyer angle. However, the relation applies along a characteristic curve, rather than throughout a plane region, as is the case in a simple wave.

Equations (2) and (9) give the characteristic paths exactly. For a given value of  $\gamma$  one curve, such as that shown in Fig. 2 for  $\gamma = \frac{7}{5}$ , serves to determine all other possible characteristics in the two family set. Once a preferred direction has been assigned, e.g., the direction of the axis of a conical nozzle, the characteristics of the  $C_+$  family which cover a meridional plane can be found from Fig. 2 by rotation of the universal curve through an arbitrary angle  $\bar{\theta}$ . The  $C_-$  family is found by first reflecting the universal curve about the  $x$ -axis and then rotating it. The resulting map is shown in Fig. 3.

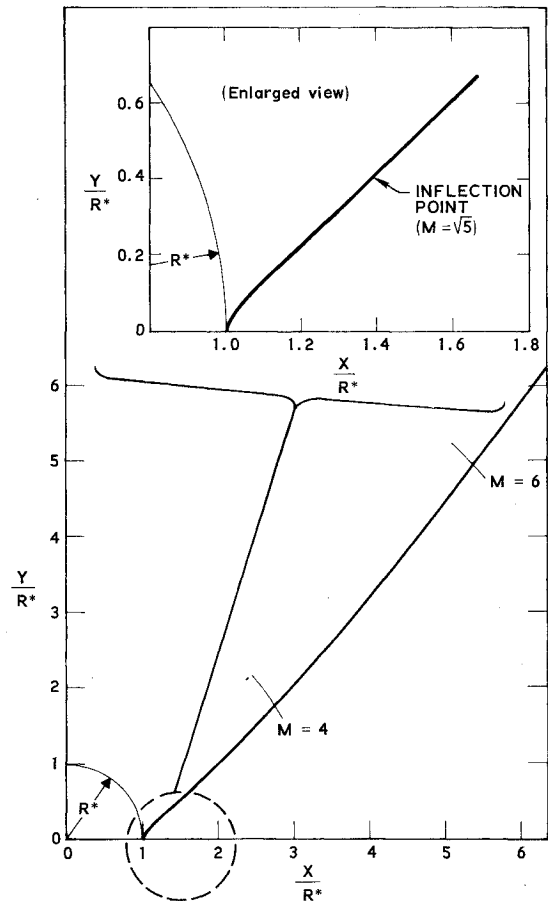


Fig. 2 Universal characteristic for spherically symmetric flow,  $\gamma = 7/5$ .

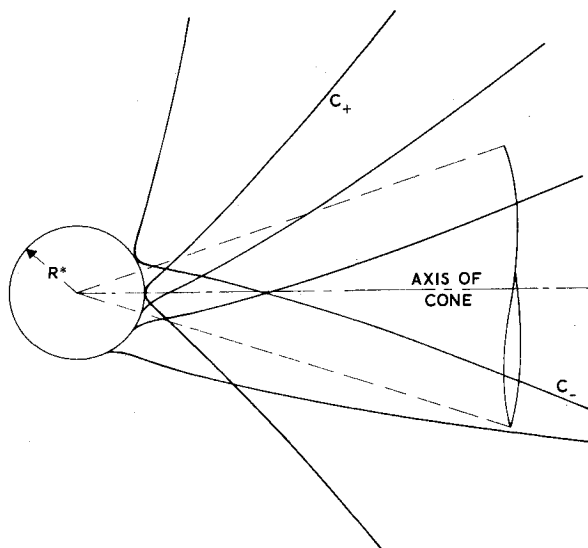


Fig. 3 Typical characteristic map,  $\gamma = 7/5$ .

A characteristic approaches a limiting slope with respect to  $\bar{\theta}$  as  $M \rightarrow \infty$ ,

$$(\theta - \bar{\theta})_{\lim} = \frac{\pi}{4} \left[ \left( \frac{\gamma + 1}{\gamma - 1} \right)^{1/2} - 1 \right] \quad (10)$$

The curvature of a characteristic has been computed from Eqs. (2) and (9) and is given by the relation

$$\kappa = \frac{d \ln R/dM - \sin \mu}{\csc \mu dR/dM} \quad (11)$$

The curvature changes sign once at the inflection point

$$M = |3/(2 - \gamma)|^{1/2} \quad (12)$$

Since the choice of the axis of symmetry for the conical cut-out flow is arbitrary, the solution is not singular on the axis.

#### Generalization to Real Gases

The preceding results may be generalized to any real gas undergoing a thermochemically frozen or equilibrium expansion.

In the latter case instead of Eq. (1) we use the differential area-velocity relation,

$$dA/A = [q^2/c^2 - 1] dq/q \quad (13)$$

where  $q$  is the velocity magnitude and  $c$  is the sound speed. Then since

$$dA/A = j dR/R \quad (14)$$

where  $j = 1$  for plane radial flow and  $j = 2$  for the spherically symmetric case, Eq. (5) yields, when integrated,

$$\theta - \theta_0 = \pm \frac{1}{j} \int_{q_0}^q \left( \frac{1}{c^2} - \frac{1}{q^2} \right)^{1/2} dq \quad (15)$$

Here the integrand is a function of both  $q$  and  $c$ , and the connection between the two in the case of a real gas must be made with the aid of a Mollier diagram or its equivalent. The integral is then evaluated numerically, holding entropy fixed (Vincenti and Kruger, pp. 189–190). The  $R$  coordinate is likewise found by integrating Eq. (13) with the aid of relation (14).

#### Summary

A simple derivation of the equations for a characteristic curve in a spherically-symmetric supersonic source flow has led to an interesting discovery. The change in streamline inclination angle  $\theta$  as a function of Mach number along the characteristic is given exactly by half the change in Prandtl-Meyer angle. The appearance of the Prandtl-Meyer function in the solution of a three-dimensional flow is believed to be a new result. In the case of radial plane flow the factor  $\frac{1}{2}$  drops out and the standard relation between  $\theta$  and  $v$  is regained. However, the relation applies along a characteristic curve rather than throughout a region, as is the case in a simple wave.

The exact solution for the characteristic curves can be used as starting data for the expansion of a conical nozzle flow around the nozzle lip. It can also be used as a check on the accuracy of approximate, finite-difference solution schemes.

#### References

- <sup>1</sup> Liepmann, H. W. and Roshko, A., *Elements of Gasdynamics*, Wiley, New York, 1957.
- <sup>2</sup> Courant, R. and Friedrichs, K. O., *Supersonic Flow and Shock Waves*, Interscience, New York, 1948.
- <sup>3</sup> Vincenti, W. G. and Kruger, C. H., *Introduction to Physical Gas Dynamics*, Wiley, New York, 1965.